ISSN 0027-1349, Moscow University Physics Bulletin, 2024, Vol. 79, Suppl. 2, pp. S731–S738. © Allerton Press, Inc., 2024.

Identification of Air Pollutants with Thermally Modulated Metal Oxide Semiconductor Gas Sensors through Machine Learning Based Response Models

I. V. Isaev[1,2,3*], K. N. Chernov[4], A. S. Sagitova[3,5], V. V. Krivetskiy[3,5], and S. A. Dolenko[1,5***]**

[1] *Skobeltsyn Institute of Nuclear Physics, Lomonosov Moscow State University, Moscow, Russia*
[2] *Kotelnikov Institute of Radio Engineering and Electronics, Russian Academy of Sciences, Moscow, Russia*
[3] *Scientific-Manufacturing Complex Technological Centre, Zelenograd, Moscow, Russia*
[4] *Physics Department, Lomonosov Moscow State University, Moscow, Russia*
[5] *Chemistry Department, Lomonosov Moscow State University, Moscow, Russia*

Received October 1, 2024; revised October 10, 2024; accepted October 20, 2024

Abstract—This study addresses the problem of environmental monitoring of air in cities and industrial areas, which consists in identification of gases and volatile organic compounds using metal oxide (MOX) semiconductor gas sensors. To provide selectivity in the detection of certain gases, the laboratory-made MOX gas sensors are operated in a modulated working temperature mode in combination with signal processing and machine learning approach to establish the response models. Six types of nonlinear operating temperature conditions—the so-called heating dynamics—were applied to twelve sensors with sensing layers of different chemical composition. Nine gases (CO, CH_4, H_2, NH_3, NO, NO_2, H_2S, SO_2, formaldehyde) in six different concentrations each were used as polluting admixtures to dry clean air. Due to the high complexity of the model describing the processes of interaction between gases and sensors, machine learning methods (logistic regression, random forest and gradient boosting) based on the use of physical experiment data were used to process the sensor response. Optimal heating dynamics and optimal machine learning methods for gas identification have been determined.

Keywords: gas sensor, machine learning methods

DOI: 10.3103/S0027134924702205

1. INTRODUCTION

Low-cost gas sensors are deemed as a perspective means of environmental monitoring with high spatio-temporal resolution [1]. Metal oxide (MOX) semiconductor resistive type sensors attract most attention in this regard due to ability of long-term continuous operation and wide spectrum of detected compounds [2]. Application of sensor arrays and signal processing allows even detection, identification and quantification of odors, which is crucial for quality-of-life assessment in highly urbanized and industrialized areas [3, 4]. The widespread practical application of such air monitoring systems requires and overcome of a current barrier—long term instability and difficulties with transferability of response models [5]. Concerning the response model transferability problem various artificial neural network architectures are applied in combination with deep learning and transfer learning approaches, which allow to significantly reduce the recalibration time and number of required data samples [6, 7]. The other approach to the model transferability problem consists in the building of the global response models, accounting for the all possible deviations of sensor properties during manufacturing [8]. The long-term response stability could be addressed with the use of machine learning approach, based on linear regression algorithms, when continuous operation time is used itself as a parameter [9]. A drift compensation without the use of the standard data samples has been suggested with the use of transfer learning as well [10]. The other machine learning approaches for metal oxide gas sensor drift compensation include extreme learning machines [11] online active or self-training models [12, 13], or deep learn-

*E-mail: isaev_igor@mail.ru
**E-mail: vkrivetsky@inorg.chem.msu.ru
***E-mail: dolenko@srd.sinp.msu.ru

ing models with automatically extracted features [14]. A combination of sensors into an array, their working temperature modulation, raw data preprocessing and machine learning based building of response model has been shown in the recent past to be fruitful in order to stabilize the sensor response against short-term effects of media fluctuations [15]. However, the influence of the working temperature modulation parameters on the response model performance were studied only in the narrow borders [16–19], and no firm connection between them were established yet. The present work addresses in the systematic fashion the question of MOX gas sensor working temperature modulation mode and its relation to the stability and quality of such response models, built upon various machine learning methods for the purpose of individual gases identification.

2. PHYSICAL EXPERIMENT

2.1. Gas Sensors Fabrication

A set of MOX gas sensors were fabricated on the basis of microelectromechanical system (MEMS) microheaters as described previously [20], with the use of a number of purposely synthesized gas sensing materials. The materials were based on nanocrystalline SnO_2 and TiO_2 semiconductor oxides, obtained via flame spray pyrolysis (FSP) route [21]. In total 12 sensors were made on the basis of pure SnO_2, SnO_2 decorated with noble metals, SnO_2 doped with Cr(III) and Nb(V) cations, SnO_2 modified with SiO_2 over the surface, including a sensor with combination of Au decoration and SiO_2 modification. These sensors are named further (1) SnO_2; (2) SnO_2–Ru; (3) SnO_2–Au; (4) SnO_2–Pd; (5) SnO_2–Pt (6) SnO_2–Cr–Nb; (7) SnO_2–SiO_2; (8) SnO_2–SiO_2–Au. TiO_2 based sensors represent n-type conducting Nb(V) doped materials with and without Au decoration, as well as *p*-type conducting Cr(III) doped materials with similar Au modification, which are named further as (9) TiO_2–Cr; (10) TiO_2–Cr–Au; (11) TiO_2–Nb–Au; (12) TiO_2–Nb. The materials were dispensed in organic binder—ethyldiglycol acetate—and deposited on the surface of the circular heated area of silicon-based MEMS element with the use of Nano-Tip HV-J microdispenser (Gesim, Germany) (Fig. 1). After the deposition the sensing elements were self-heated by MEMS-microheater up to 500°C and kept for 10 h for binder complete evaporation and MOX porous sensing layer formation.

2.2. Gas Sensor Experiment and Data Collection

The electrical resistance of a gas sensing semiconductor element depends, on the one side, on the working temperature (due to thermal activation of charge carriers and their transfer into the conduction band), and on the other side—on the rate of chemical reactions on the metal oxide surface. The first type of contribution, if big enough, may obscure the resistance changes due to gas sensor process. Thus, the amplitude and temporal characteristics of the working temperature modulation mode of the sensing element may affect the applicability of the obtained sensor response for a response model built within machine learning approach. To systematically study this issue, six working temperature operating conditions (the so-called heating dynamics) were considered in the present study (Fig. 2):

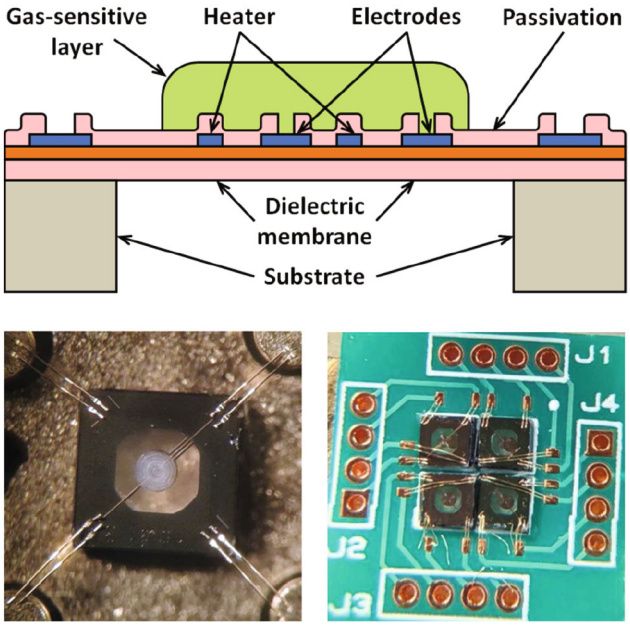

Fig. 1. Top—schematic design of a semiconductor gas sensor; bottom left—MEMS-microhotplate with printed SnO_2 sensing layer, fixed in TO-5 package; bottom right—a set of four sensors, fixed on a printed circuit board (PCB).

- Two linear dynamics with different cycle lengths—*linear short (LS)* and *linear long (LL)*;
- Two dynamics with a stepwise increase and decrease in temperature—*step up (SU)* and *step down (SD)*;
- Two dynamics with a stepwise increase and decrease in temperature and short-term pulsed temperature jumps to maximum working temperature, which is associated with rapid desorption of products of chemical interaction from metal oxide surface—*step up pulse (SUP)* and *step down pulse (SDP)*.

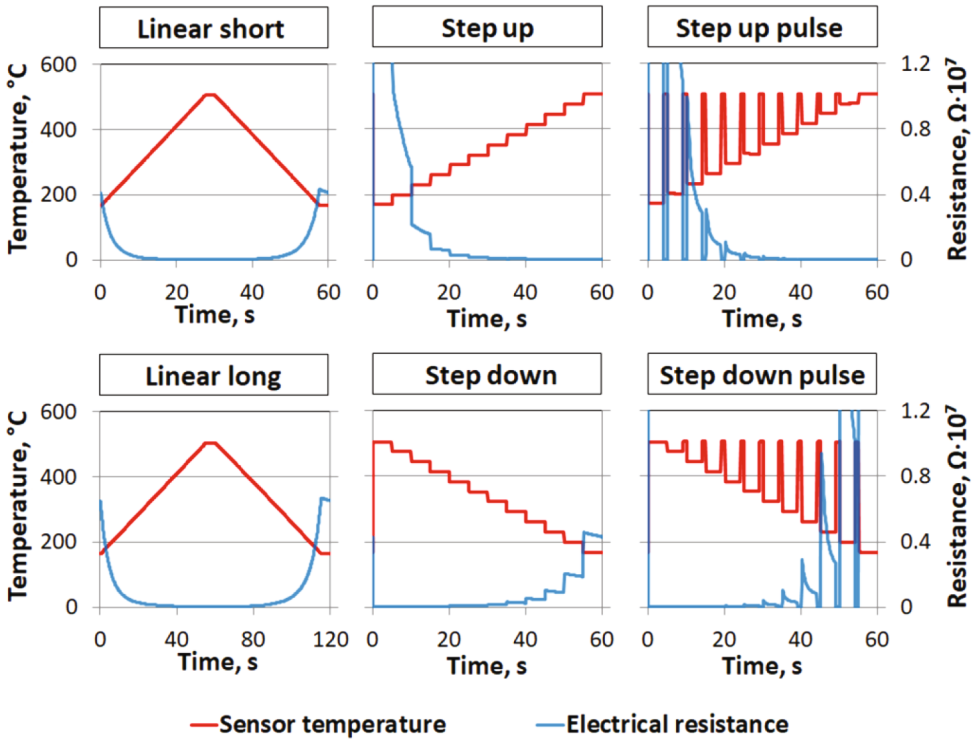

Fig. 2. Heating dynamics and sensor responses.

To determine the optimal modulation mode of operating temperature of gas sensors, the response forms of the 12 sensors were collected in an atmosphere of dry clean air, as well as in dry air with an admixture of one of nine gases—CO, H_2, CH_4, NH_3, NO, NO_2, H_2S, SO_2, HCOH (formaldehyde). Only clean air or admixture of only one gas was present in the sensor chamber at a time. Each gas has been flown through the sensor chamber in a constant flow mode in six different concentrations in different consecutive periods of time. The same gas flow program has been repeated for the each of six heating dynamics, which were mentioned above. In each series of measurements (Fig. 3), the experimental setup was first purged and then a gas was supplied. In this case, the gas concentration was maintained constant for a certain number of heating dynamics cycles. Each concentration value was maintained within the same number of cycles and was repeated twice in one series of experiments.

3. APPLICATION OF MACHINE LEARNING METHODS

3.1. Data Preprocessing

To implement the application of machine learning methods to the initial data (Fig. 3, left) of chemical sensor responses, data preparation and preprocessing was carried out, which included the following steps:

1. Converting data into the format: “1 cycle of temperature modulation—1 pattern of a training sample.”

2. Replacing sensor response values above 10^{10} Ω with a fixed value of 10^{10}Ω, and response values below 10 Ω with a fixed value of 10 Ω.

3. Exclusion of data sections where the experimental setup was purged: the first several cycles in each experiment.

4. Elimination of the first several cycles after changing the concentration (5 for short temperature dynamics, 3 for long) and several cycles immediately before changing the concentration (3 for short temperature dynamics, 2 for long) (Fig. 3, right).

5. Taking decimal logarithm of sensory response.

6. Binary encoding of classes: 0—absence of gas, 1—presence of gas.

7. Splitting the resulting data set into training and test sets. It was carried out in a stratified version (Fig. 3, right): from each area with a fixed concentration of the gas in question, the first m cycles were selected into the training set and the subsequent n cycles were selected into

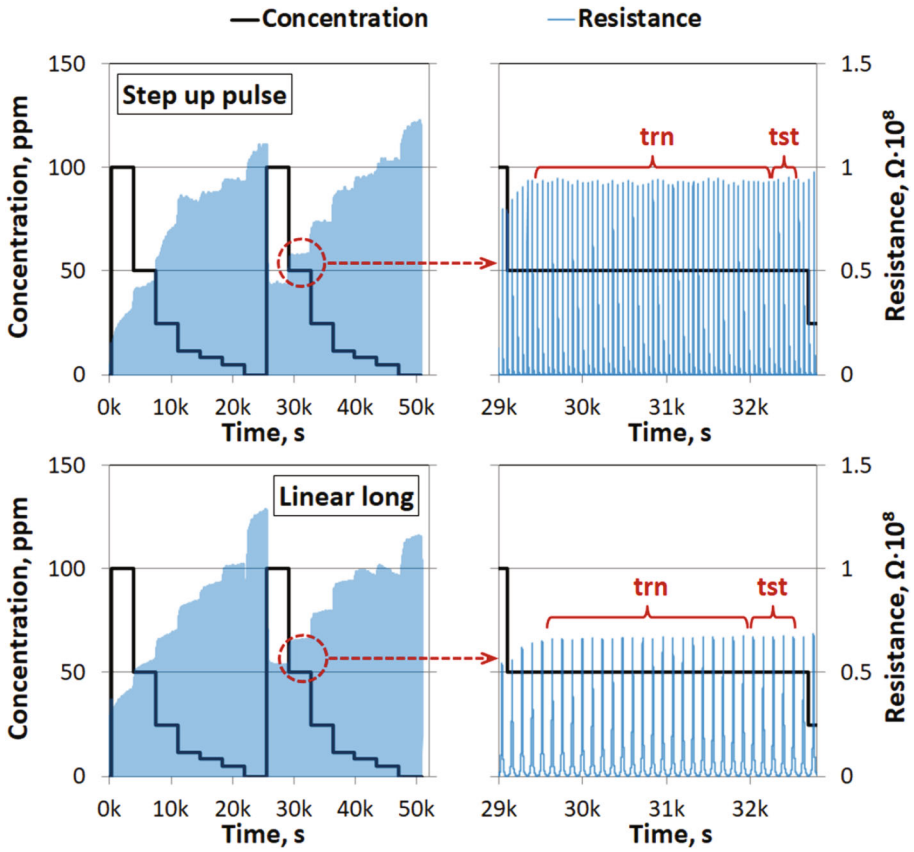

Fig. 3. Left—the original data of sensor response, right—splitting into training and test subsets.

RF - LL	Sensor No												Sensor No											
Gas	1	2	3	4	5	6	7	8	9	10	11	12	1	2	3	4	5	6	7	8	9	10	11	12
CH_4	1	1	1	1	1	1	1	1	0.957	0.884	1	1	0	0	0	0	0	0	0	0	0	0.007	0	0
CO	1	1	1	1	1	0.997	1	1	0.967	1	0.957	1	0	0	0	0	0	0.008	0	0	0.016	0	0	0
H_2	1	1	1	1	1	1	1	1	0.945	1	1	0.762	0	0	0	0	0	0	0	0	0.01	0	0	0
H_2S	1	1	1	1	1	1	1	1	1	1	1	1	0	0	0	0	0	0	0	0	0	0	0	0
HCOH	1	1	1	1	1	0.984	1	1	1	1	0.909	1	0	0	0	0	0	0.022	0	0	0	0	0	0
NH_3	1	1	1	1	1	1	1	1	1	0.98	1	0.998	0	0	0	0	0	0	0	0	0	0.005	0	0.004
NO	0.957	0.927	1	1	0.955	1	0.997	0.997	1	1	0.896	0.957	0	0.007	0	0	0.007	0	0.005	0.005	0	0	0.073	0
NO_2	0.814	0.949	0.833	0.909	0.992	0.85	0.971	0.903	0.985	1	1	0.651	0.006	0.01	0.01	0	0.008	0.015	0.005	0.056	0.007	0	0	0.016
SO_2	0.794	0.854	0.854	0.842	0.831	0.701	0.819	0.811	0.945	0.94	0.706	0.772	0.025	0.004	0.004	0.01	0.016	0.007	0.02	0.002	0.017	0.02	0.028	0.007

Fig. 4. F1-score values for random forest algorithm applied to sensor data obtained through "linear long" heating dynamic for various gases and various sensors: Left—F1-score averaged over 5 random seeds, right—F1-score standard deviation.

the test set ($m : n = 47 : 5$—for short temperature dynamics, $m : n = 20 : 5$—for long temperature dynamics), then the procedure was repeated for other sections with a fixed concentration.

3.2. Statement of the Computational Experiment

In this study, we considered a *binary classification problem* that involved determining the presence of a specific gas using data from a single physical experiment with a specific heating dynamic. In each computational experiment, data from only one sensor was used. So, the following number of problem statements were considered:

*9 determined gases * 6 heating dynamics**
**12 sensors = 648 problem statements*

In each separate computational experiment, the problem of determining presence/absence of only one gas was solved based on the sensor resistance values during one cycle of heating dynamics (1201 resistance values for linear long heating dynamics, 601 values for other heating dynamics).

3.3. Using Machine Learning Methods

Machine learning methods used were logistic regression (without regularization and with L1 and L2

LR	Sensor No											
Gas	1	2	3	4	5	6	7	8	9	10	11	12
CH_4	1	1	1	1	1	0.981	1	1	0.926	0.944	0.985	0.983
CO	1	1	1	1	1	0.999	1	1	0.962	0.972	0.994	0.999
H_2	1	1	1	1	1	0.997	1	1	0.95	0.996	1	0.971
H_2S	1	1	1	1	1	1	1	1	1	1	1	0.999
HCOH	1	1	1	1	0.999	1	1	1	0.99	0.978	0.976	0.999
NH_3	1	1	1	1	1	1	1	1	0.996	0.994	1	0.99
NO	1	1	1	1	1	0.999	1	1	1	1	0.996	0.993
NO_2	1	1	1	1	0.996	0.981	1	1	0.973	0.987	0.956	0.977
SO_2	0.99	0.987	0.996	0.98	1	0.971	0.983	1	0.971	0.957	0.931	0.984

LR	Heat dynamics					
Gas	LL	LS	SD	SU	SDP	SUP
CH_4	0.988	0.981	0.978	0.991	0.984	0.988
CO	0.993	1	0.992	0.997	0.994	0.987
H_2	0.984	0.996	0.994	0.994	0.996	0.993
H_2S	1	1	0.999	1	1	1
HCOH	0.999	0.994	0.993	0.996	0.997	0.993
NH_3	1	1	0.998	0.998	0.995	0.999
NO	0.999	1	0.996	1	0.999	0.999
NO_2	0.976	0.997	0.971	0.997	0.996	0.998
SO_2	0.96	1	0.999	0.968	0.95	0.998

LR-L1	Sensor No											
Gas	1	2	3	4	5	6	7	8	9	10	11	12
CH_4	1	1	1	1	1	0.708	1	1	0.627	0.554	0.739	0.973
CO	0.947	0.945	0.963	0.949	0.999	0.921	0.95	0.993	0.785	0.827	0.931	0.972
H_2	1	1	1	1	1	1	1	1	0.572	0.799	1	0.825
H_2S	1	1	1	1	1	1	1	1	0.957	0.945	1	1
HCOH	0.994	0.997	1	1	0.991	0.873	0.999	0.999	0.817	0.834	0.804	0.874
NH_3	0.967	0.98	0.954	0.947	0.959	0.928	0.965	0.973	0.934	0.939	0.948	0.966
NO	0.996	1	1	0.993	0.999	0.997	0.996	0.998	0.987	0.997	0.898	0.946
NO_2	0.954	0.973	0.982	0.964	0.97	0.849	0.969	0.97	0.839	0.842	0.821	0.881
SO_2	0.875	0.739	0.899	0.87	0.881	0.845	0.857	0.902	0.672	0.809	0.779	0.893

LR-L1	Heat dynamics					
Gas	LL	LS	SD	SU	SDP	SUP
CH_4	0.74	0.899	0.923	0.907	0.928	0.904
CO	0.906	0.985	0.95	0.914	0.917	0.918
H_2	0.894	0.93	0.936	0.979	0.926	0.933
H_2S	0.994	0.996	1	0.997	0.986	0.978
HCOH	0.934	0.944	0.96	0.913	0.931	0.909
NH_3	0.94	0.964	0.977	0.95	0.931	0.967
NO	0.963	0.981	0.987	0.988	0.993	0.991
NO_2	0.828	0.985	0.879	0.958	0.926	0.932
SO_2	0.635	0.989	0.979	0.747	0.713	0.948

LR-L2	Sensor No											
Gas	1	2	3	4	5	6	7	8	9	10	11	12
CH_4	1	1	1	1	1	0.871	1	1	0.817	0.797	0.93	0.985
CO	0.999	0.997	1	1	1	0.967	0.997	1	0.861	0.908	0.977	0.997
H_2	1	1	1	1	1	1	1	1	0.804	0.909	1	0.943
H_2S	1	1	1	1	1	1	1	1	0.991	0.996	1	0.997
HCOH	1	1	1	1	0.997	0.979	1	1	0.923	0.921	0.871	0.957
NH_3	0.994	0.999	0.999	0.996	0.997	0.982	0.996	0.997	0.975	0.983	0.991	0.983
NO	1	1	1	0.993	0.999	0.997	1	0.999	0.999	1	0.965	0.988
NO_2	0.987	0.999	1	0.993	0.991	0.935	1	0.999	0.911	0.925	0.883	0.944
SO_2	0.934	0.928	0.961	0.925	0.967	0.888	0.93	0.959	0.866	0.855	0.807	0.902

LR-L2	Heat dynamics					
Gas	LL	LS	SD	SU	SDP	SUP
CH_4	0.973	0.956	0.954	0.946	0.945	0.926
CO	0.986	0.985	0.981	0.963	0.968	0.969
H_2	0.978	0.983	0.97	0.97	0.961	0.965
H_2S	1	1	0.999	1	0.996	0.997
HCOH	0.989	0.976	0.98	0.96	0.959	0.959
NH_3	0.996	1	0.994	0.995	0.965	0.996
NO	0.996	0.994	0.99	0.995	0.998	0.996
NO_2	0.945	0.996	0.916	0.994	0.975	0.957
SO_2	0.865	0.995	0.995	0.826	0.811	0.969

RF	Sensor No											
Gas	1	2	3	4	5	6	7	8	9	10	11	12
CH_4	0.993	0.976	0.967	0.993	0.993	0.874	0.993	0.986	0.934	0.906	0.979	0.93
CO	1	1	1	0.992	1	0.954	0.999	0.997	0.944	0.959	0.975	0.972
H_2	1	1	1	1	1	0.994	1	1	0.924	0.993	1	0.908
H_2S	1	1	1	1	1	1	1	1	1	1	1	0.978
HCOH	1	0.998	0.999	0.996	1	0.943	0.999	1	0.978	0.981	0.821	0.883
NH_3	0.995	0.999	1	1	0.997	0.993	0.995	0.994	0.977	0.98	0.995	1
NO	0.985	0.979	0.991	0.989	0.99	0.95	0.966	0.968	1	1	0.956	0.961
NO_2	0.953	0.964	0.961	0.95	0.99	0.928	0.985	0.969	0.967	0.981	0.935	0.833
SO_2	0.885	0.902	0.892	0.914	0.9	0.891	0.844	0.858	0.948	0.919	0.826	0.903

RF	Heat dynamics					
Gas	LL	LS	SD	SU	SDP	SUP
CH_4	0.987	0.927	0.939	0.978	0.957	0.974
CO	0.993	1	0.99	0.972	0.961	0.979
H_2	0.976	0.989	0.974	0.988	0.994	0.989
H_2S	1	1	0.989	1	1	1
HCOH	0.991	0.978	0.979	0.929	0.974	0.948
NH_3	0.998	0.999	0.998	0.997	0.976	0.994
NO	0.974	0.98	0.99	0.965	0.986	0.974
NO_2	0.905	0.978	0.95	0.946	0.988	0.941
SO_2	0.822	1	1	0.771	0.777	0.971

GB	Sensor No											
Gas	1	2	3	4	5	6	7	8	9	10	11	12
CH_4	1	1	0.993	1	1	0.956	1	1	0.972	0.97	0.992	0.967
CO	1	1	1	1	1	1	1	1	0.992	0.998	0.99	0.999
H_2	1	1	1	1	1	1	1	1	0.976	1	1	0.988
H_2S	1	1	1	1	1	1	1	1	1	1	1	0.999
HCOH	1	1	1	1	1	0.987	1	1	1	0.999	0.959	0.976
NH_3	1	1	1	1	1	0.999	1	1	0.997	0.999	1	1
NO	0.992	0.998	0.999	0.991	0.985	0.981	0.98	0.991	1	1	0.985	0.982
NO_2	0.98	0.993	0.987	0.984	0.989	0.979	0.989	0.988	0.981	0.994	0.964	0.949
SO_2	0.981	0.972	0.978	0.999	0.983	0.976	0.981	0.976	0.977	0.979	0.977	0.969

GB	Heat dynamics					
Gas	LL	LS	SD	SU	SDP	SUP
CH_4	0.992	0.98	0.982	0.994	0.984	0.994
CO	0.998	1	1	0.996	0.996	0.999
H_2	0.993	0.996	0.998	0.997	0.998	1
H_2S	1	1	1	1	1	1
HCOH	0.999	0.996	0.997	0.985	0.994	0.99
NH_3	1	1	0.999	1	0.999	1
NO	0.986	0.992	1	0.98	0.993	0.992
NO_2	0.981	0.972	0.991	0.981	0.993	0.969
SO_2	0.95	1	1	0.968	0.956	0.999

Fig. 5. Averaged values of sensor response models performance (F1-score) for various gases and various sensors: left—averaged over sensors, right—averaged over types of heating dynamics. Different tables contain results for different algorithms; algorithm type is specified in the upper left corner of each table.

regularization), random forest, and gradient boosting. Programming was carried out in Python language using the scikit-learn (v.1.5) [22] machine learning library. For each method a grid search was carried out on a limited set of problems in order to find the optimal training parameters. In this case, one problem from each heating dynamics with different sensors and gases was considered. As a result, the following consensus parameters were chosen for all subsequent experiments:

- *Logistic regression without regularization (LR)*: solver—"newton-cg"; maximum number of iterations—250; tolerance for the optimization—0.0001.
- *LR with L1 regularization (LR-L1)*: inverse of regularization strength—1.0; solver—

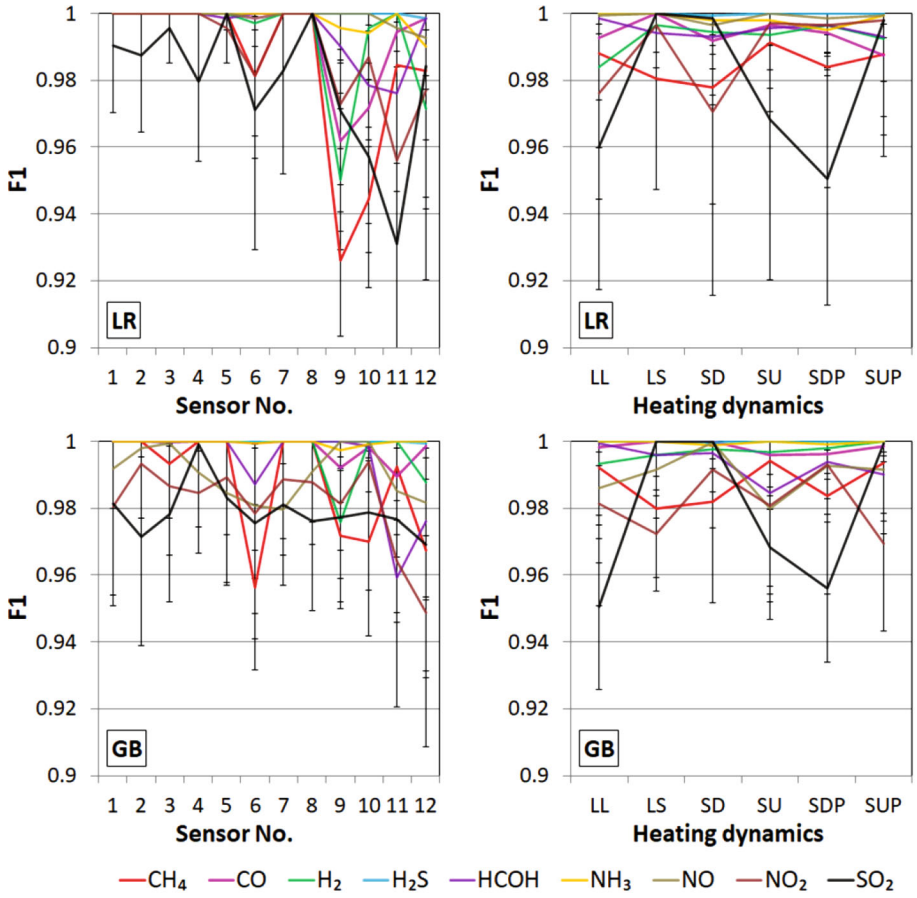

Fig. 6. Averaged values of sensor response models performance (F1-score): left—averaged over sensors, right—averaged over types of heating dynamics. Top—linear regression, bottom—gradient boosting. Multiple cut-offs on the whiskers correspond to the error values for various gases.

"liblinear" ; maximum number of iterations—250; tolerance for the optimization—0.0001.

- *LR with L2 regularization (LR-L2)*: inverse of regularization strength—10.0; solver—"lbfgs" ; maximum number of iterations—250; tolerance for the optimization—0.0001.

- *Gradient boosting (GB)* over decision trees (DT): number of DT—100; DT depth—3; learning rate—0.01; number of features to consider when looking for the best split in the nodes of the DT—$\log_2(n)$, where n is the total number of features; early stopping after 250 iterations without validation loss improving; tolerance for the early stopping—0.001.

- *Random forest (RF)*: number of DT—50; DT depth—2, fraction of features to consider when looking for the best split in the nodes of the DT—sqrt(n), where n is the total number of features.

For each method 5 models with different random initializations were trained in each experiment. The application results statistics were averaged.

4. RESULTS

As an indicator of the quality of binary classification in this study, the F1-score was considered. Since the number of patterns corresponding to the presence of gas is six times greater than the number of patterns corresponding to the absence of gas, the trivial solution model (all patterns are assigned to one larger class) corresponds to F1-score value of 0.923. This should be taken into account when analyzing the following results.

For each specific problem, the solution results were obtained by all considered machine learning methods (an example is presented at Fig. 4). For ease of analysis and identification of characteristic general patterns, the obtained results were averaged over all sensors and over all heating dynamics (Figs. 5 and 6). The observed results could be generalized in the following points:

- Logistic regression without regularisation performed better than regression with L1 and L2 regularisation. Gradient boosting was more efficient than the decision tree algorithm. These two algorithms—gradient boosting and logistic regression without regularisation—gave results close in performance.

- Application of L1 regularisation led to the worst performance of the response model in the present study. Compared to the L2 regularisation, which has the second worst performance, and which minimizes the contribution of the weak features, the L1 regularisation makes them null. This consideration gives rise to a conclusion, that the task of the binary classification requires as many features of the data sample as possible.

- SnO_2-based sensors performed generally better, than TiO_2-based ones, which correlates with their better sensitivity—higher response values. However, application of gradient boosting algorithm allowed to alleviate this issue. The outlying problems with 6-th sensor, made of Cr(III) and Nb(V) doped SnO_2, visible for all algorithms applied, indicate the instability of this sensor.

- Generally reducing gases are better recognized, than oxidizing ones (NO, NO_2, SnO_2). While in the case of SO_2 this result could be anticipated due to very low concentrations of this gas in the flow of dry clean air, for other two gases this observation requires further clarification.

- Comparison of the heating dynamics allows us to assume that slower heating and cooling is better than faster one (LL vs LS), heating up gives more features, than cooling down (SU and SUP vs SD and SDP); however, the latter tendency is not very profound.

5. CONCLUSIONS

Based on the results of the study, the following conclusions were made:

- Increase in the absolute value of sensor response is beneficial for machine learning sensor response model for gas presence recognition.

- Logistic regression and gradient boosting based models are best performing, able to compensate for poor sensor response and for response drift over time.

- Testing of these results on the independent datasets is required in the future studies.

FUNDING

This study has been performed at the expense of the Russian Science Foundation, grant no. 22-19-00703, https://rscf.ru/en/project/22-19-00703/.

CONFLICT OF INTEREST

The authors of this work declare that they have no conflicts of interest.

REFERENCES

1. O. Alsamrai, M. D. Redel-Macias, S. Pinzi, and M. P. Dorado, Sustainability **16**, 4353 (2024). https://doi.org/10.3390/su16114353
2. A. Milone, A. G. Monteduro, S. Rizzato, A. Leo, C. Di Natale, S. S. Kim, and G. Maruccio, Adv. Sustainable Syst. **7**, 2200083 (2023). https://doi.org/10.1002/adsu.202200083
3. S. Dimitriadou, P. A. Kokkinos, G. Z. Kyzas, and I. K. Kalavrouziotis, Sci. Total Environ. **949**, 174966 (2024). https://doi.org/10.1016/j.scitotenv.2024.174966
4. A. Rabehi, H. Helal, D. Zappa, and E. Comini, Appl. Sci. **14**, 4506 (2024). https://doi.org/10.3390/app14114506
5. A. T. John, K. Murugappan, D. R. Nisbet, and A. Tricoli, Sensors **21**, 2271 (2021). https://doi.org/10.3390/s21072271
6. Ya. Robin, J. Amann, P. Goodarzi, T. Schneider, A. Schütze, and Ch. Bur, Atmosphere **13**, 1614 (2022). https://doi.org/10.3390/atmos13101614
7. D. Arendes, Ya. Robin, J. Amann, A. Petto, A. Schütze, and Ch. Bur, in *2024 IEEE International Symposium on Olfaction and Electronic Nose (ISOEN), Grapevine, TX, 2024* (IEEE, 2024), p. 1. https://doi.org/10.1109/isoen61239.2024.10556179
8. A. Miquel-Ibarz, J. Burgués, and S. Marco, Sens. Actuators, B **350**, 130769 (2022). https://doi.org/10.1016/j.snb.2021.130769
9. M. Levy Zamora, C. Buehler, H. Lei, A. Datta, F. Xiong, D. R. Gentner, and K. Koehler, ACS ES amp;T Engineering **2**, 780 (2022). https://doi.org/10.1021/acsestengg.1c00367
10. Z. Jiang, P. Xu, Yo. Du, F. Yuan, and K. Song, Sensors **21**, 3403 (2021). https://doi.org/10.3390/s21103403
11. P. Das, A. Manna, and S. Ghoshal, in *2020 International Conference on Renewable Energy Integration into Smart Grids: A Multidisciplinary Approach to Technology Modelling and Simulation (ICREISG), Bhubaneswar, India, 2020* (IEEE, 2020), p. 197. https://doi.org/10.1109/icreisg49226.2020.9174554

12. X. Dong, Sh. Han, A. Wang, and K. Shang, Chemosensors **9**, 353 (2021). https://doi.org/10.3390/chemosensors9120353
13. T. Liu, D. Li, J. Chen, Ya. Chen, T. Yang, and J. Cao, Sensors **18**, 4028 (2018). https://doi.org/10.3390/s18114028
14. Q. Liu, X. Hu, M. Ye, X. Cheng, and F. Li, Int. J. Intell. Syst. **30**, 907 (2015). https://doi.org/10.1002/int.21731
15. V. V. Krivetskiy, M. D. Andreev, A. O. Efitorov, and A. M. Gaskov, Sens. Actuators, B **329**, 129187 (2021). https://doi.org/10.1016/j.snb.2020.129187
16. D. Di Giuseppe, A. Catini, E. Comini, D. Zappa, C. Di Natale, and E. Martinelli, Sens. Actuators, B **333**, 129509 (2021). https://doi.org/10.1016/j.snb.2021.129509
17. R. Gosangi and R. Gutierrez-Osuna, Sens. Actuators, B **185**, 201 (2013). https://doi.org/10.1016/j.snb.2013.04.056
18. A. Vergara, E. Llobet, J. Brezmes, X. Vilanova, P. Ivanov, I. Gracia, C. Cane, and X. Correig, IEEE Sens. J. **5**, 1369 (2005). https://doi.org/10.1109/jsen.2005.855605
19. F. Palacio, J. Fonollosa, J. Burgues, J. M. Gomez, and S. Marco, IEEE Access **8**, 70938 (2020). https://doi.org/10.1109/access.2020.2987066
20. M. Andreev, V. Platonov, D. Filatova, E. Galitskaya, S. Polomoshnov, S. Generalov, A. Nikolaeva, V. Amelichev, O. Zhdaneev, V. Krivetskiy, and M. Rumyantseva, Sensors **21**, 7297 (2021). https://doi.org/10.3390/s21217297
21. V. Krivetskiy, K. Zamanskiy, A. Beltyukov, A. Asachenko, M. Topchiy, M. Nechaev, A. Garshev, A. Krotova, D. Filatova, K. Maslakov, M. Rumyantseva, and A. Gaskov, Nanomaterials **9**, 728 (2019). https://doi.org/10.3390/nano9050728
22. F. Pedregosa, G. Varoquaux, A. Gramfort, V. Michel, B. Thirion, O. Grisel, M. Blondel, P. Prettenhofer, R. Weiss, V. Dubourg, J. Vanderplas, A. Passos, D. Cournapeau, M. Brucher, M. Perrot, and É. Duchesnay, J. Mach. Learn. Res. **12**, 2825 (2011). https://doi.org/10.5555/1953048.2078195